

Simulation and Control of a Rotary Inverted Pendulum

Carlos Wellington Passos Gonçalves, carlosoleto@gmail.com

Geovany Araújo Borges, gaborges@ene.unb.br

Laboratório de Robótica e Automação (LARA), Departamento de Engenharia Elétrica (ENE), Universidade de Brasília (UnB), Brasília, Brazil

Abstract. *The rotary inverted pendulum is a control design problem which covers many research topics. Due to its intrinsic non-linearity, chaotic movement, and underactuated control, it is an ideal experiment for the application of modern control techniques. In order to build a physical implementation of its system, one needs to previously study its dynamics and obtain an accurate computational simulation to guide this task. In this paper, a simulator provides the user a friendly interface in which a customized physical implementation of the double inverted pendulum can be studied. The user can choose among different control techniques, namely classical space-state control and optimal LQG control using a Kalman filter. The simulation is useful in determining the requirements of torque and controllability for the system according to the choice of link lengths and materials. Such requirements can only be determined using a simulation of the system dynamic model. The paper presents a complete description of the pendulum dynamic model, control design and physical implementation aided through the simulated model.*

Keywords: *rotary inverted pendulum, control system design, computer-aided design*

1. INTRODUCTION

Throughout the world, control theory laboratories have didactic experiments in order to permit that theoretical approaches to control a system can be actually used in real life. The research in control theory also needs experiments where the new techniques can be applied. So, there is a growing idea of creating laboratories where, with few control experiments, many research topics can be studied (Horáček, 2000).

A very simple system, often used in control laboratories, is the inverted pendulum. It has a very simple mechanical system, but its non-linearity and chaotic movement brings a great challenge to the controlling task (Zhou and Whiteman, 1996) and (Stachowiak and Okada, 2006). The most common inverted pendulum experiment is the *cart-pendulum*, which is a pole that must be balanced by the movement of a cart underneath it (Horáček, 2000). A trickier experiment would be a rotary inverted pendulum, also called *pendubot* (Spong and Block, 1995). A rotary inverted pendulum has even more non-linear dynamics, and with it can be studied the task of balancing the upper pole and even swinging it up from below (Awtar et al., 2002). Fig 1 shows the rotary inverted pendulum under development at Laboratório de Robótica e Automação (LARA) in UnB.



Figure 1. Physical implementation of a rotary inverted pendulum built at LARA in UnB.

In order to build a rotary inverted pendulum, there must be some information about which could be the best combination of physical parameters to create a feasible control experiment. In order to obtain such design parameters, there must be a mathematical modeling of the system. From such model, a simulator can be built in which any closed-loop control configuration can be studied. As a result, good combination of parameters could be used in a physical implementation.

One of the most important information acquired from the simulations is the magnitude of the control signal. This information would be the difference in utilizing a very powerful and expensive motor that would not work in its full capacity, and another one that would not be capable of controlling the rotary inverted pendulum.

With a simulation that aids choosing the right parameters to a physical implementation of any system, money and priceless work-time can be saved. The major contribution of this paper must be the encouragement of this way of project development.

This paper is organized as follows. Section 2 contains the description of the rotary inverted pendulum and its mathematical model. In Section 3 a proposed LQG control is analyzed and implemented in Section 4 with the chosen simulation parameters. Section 5 has the simulation results and in Section 6 are the conclusions obtained from this paper. The references utilized are in Section 7.

2. SYSTEM DESCRIPTION AND MODELLING

The rotary inverted pendulum here studied can be reduced to the schematic model shown in Fig. 2. On the joint represented by the point **O** is placed the DC motor, the system's actuator. The system is underactuated since the other joint at point **A** there is no actuator. In this way, with only one control input, both angles from the poles that compose the pendulum must be controlled.

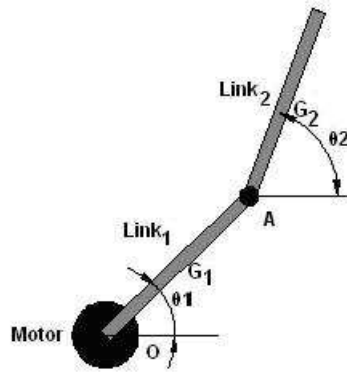


Figure 2. Schematic model from rotary inverted pendulum.

In order to obtain the mathematical model of a rotary inverted pendulum, one approach consists in analyzing it through free body diagrams (Merian and Kraige, 1999). The Figure 3 below shows how it can be done. Are represented the control input of the system, u , the weight force from each pendulum's poles, P_1 and P_2 , the damping torques from each pendulum's joints, D_1 and D_2 with respectively damping coefficients d_1 and d_2 , the internal forces on point **A**, A_x and A_y , and finally the angles from each pole, θ_1 and θ_2 .

Using momentum, forces on horizontal and vertical axis equations, the problem can not be fully answered, so there must be an analysis of the relative acceleration between points **O** and **A**, and the relative acceleration between point **O** and the center of mass from Link₂ (Merian and Kraige, 1999) and (Zhou and Whiteman, 1996). The following system will then be obtained.

$$\alpha_1 = \frac{(m_2 l_2^2 + 4I_{G2})N_1 - (2m_2 l_1 l_2 \cos(\theta_2 - \theta_1))N_2}{D}, \quad (1)$$

$$\alpha_2 = \frac{-(2m_2 l_1 l_2 \cos(\theta_2 - \theta_1))N_1 + 4(m_2 l_1^2 + I_{O1})N_2}{D}, \quad (2)$$

$$\text{where, } N_1 = -u + d_1 \omega_1 - d_2 (\omega_2 - \omega_1) + \frac{1}{2} m_1 l_1 g \cos(\theta_1) + m_2 l_1 \cos(\theta_1) - \frac{1}{2} m_2 l_1 l_2 \omega_2^2 \sin(\theta_2 - \theta_1), \quad (3)$$

$$N_2 = d_2 (\omega_2 - \omega_1) + \frac{1}{2} m_2 l_2 g \cos(\theta_2) + \frac{1}{2} m_2 l_1 l_2 \omega_1^2 \sin(\theta_2 - \theta_1), \quad (4)$$

$$D = -m_2^2 l_1^2 l_2^2 - 4m_2 l_1^2 I_{G2} - I_{O1} m_2 l_2^2 - 4I_{O1} I_{G2} + m_2^2 l_1^2 l_2^2 \cos^2(\theta_2 - \theta_1). \quad (5)$$

For each Link _{i} , $i = 1, 2$, there are represented its mass (m_i), length (l_i), angular speed (ω_i) and angular acceleration (α_i). The coefficients I_{G2} and I_{O1} correspond respectively to the inertia momentum from Link₂ through its center of mass, and to the inertia momentum from Link₁ through the point **O**.

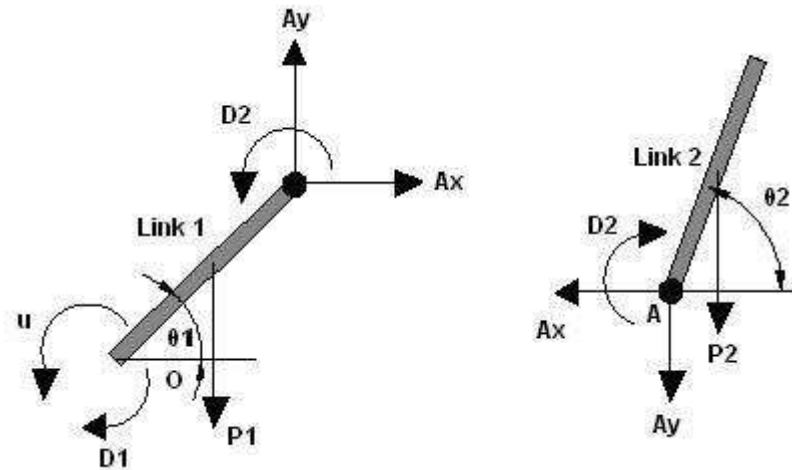


Figure 3. Free body diagrams for both Link₁ and Link₂.

Considering the state space variables θ_1 , $\dot{\theta}_1$, θ_2 and $\dot{\theta}_2$, and solving the system from Eqs. (1) and (2), are obtained the dynamic equations for the rotary inverted pendulum:

$$\dot{\mathbf{x}} = \begin{bmatrix} \dot{x}_1 \\ \dot{x}_2 \\ \dot{x}_3 \\ \dot{x}_4 \end{bmatrix} = \begin{bmatrix} \dot{\theta}_1 \\ \ddot{\theta}_1 \\ \dot{\theta}_2 \\ \ddot{\theta}_2 \end{bmatrix} = \mathbf{f}(\mathbf{x}, u) = \begin{bmatrix} f_1(\mathbf{x}, u) \\ f_2(\mathbf{x}, u) \\ f_3(\mathbf{x}, u) \\ f_4(\mathbf{x}, u) \end{bmatrix}, \quad (6)$$

$$\text{where, } \dot{x}_1 = x_2, \quad (7)$$

$$\dot{x}_2 = \frac{-12N_3}{l_1^2(12m_2 + 4m_1 - 9m_2 \cos^2(x_3 - x_1))} + \frac{18 \cos(x_3 - x_1)N_4}{l_1 l_2(12m_2 + 4m_1 - 9m_2 \cos^2(x_3 - x_1))}, \quad (8)$$

$$\dot{x}_3 = x_4, \quad (9)$$

$$\dot{x}_4 = \frac{18 \cos(x_3 - x_1)N_3}{l_1 l_2(12m_2 + 4m_1 - 9m_2 \cos^2(x_3 - x_1))} - \frac{12(3m_2 + m_1)N_4}{m_2 l_2^2(12m_2 + 4m_1 - 9m_2 \cos^2(x_3 - x_1))}, \quad (10)$$

$$\text{where, } N_3 = -u + d_1 x_2 - d_2(x_4 - x_2) + \frac{1}{2}m_1 l_1 g \cos(x_1) + m_2 l_1 \cos(x_1) - \frac{1}{2}m_2 l_1 l_2 x_4^2 \sin(x_3 - x_1), \quad (11)$$

$$N_4 = d_2(x_4 - x_2) + \frac{1}{2}m_2 l_2 g \cos(x_3) + \frac{1}{2}m_2 l_1 l_2 x_2^2 \sin(x_3 - x_1). \quad (12)$$

This non-linear model will be used during the system's simulation to obtain its motion. A fourth order Runge-Kutta algorithm solves numerically this system of differential equations, providing an accurate approximation for the rotary inverted pendulum behavior (Press et al., 1992).

In order to utilize the state space control, the system must be linearized at an equilibrium point (x_0, u_0) , where $\mathbf{f}(x_0, u_0) = 0$ (Franklin et al., 1998).

Linearizing and having the output \mathbf{y} for both θ_1 and θ_2 , is obtained the state space representation below:

$$u = u_0 + \delta u \quad (13)$$

$$\mathbf{x} = \mathbf{x}_0 + \delta \mathbf{x} \quad (14)$$

$$\mathbf{y} = \mathbf{y}_0 + \delta \mathbf{y} \quad (15)$$

$$\dot{\delta \mathbf{x}} = \mathbf{F} \delta \mathbf{x} + \mathbf{G} \delta u, \quad (16)$$

$$\delta \mathbf{y} = \mathbf{H}(\delta \mathbf{x}), \quad (17)$$

$$\text{where, } \mathbf{y} = \begin{bmatrix} x_1 \\ x_3 \end{bmatrix} = \mathbf{H} \begin{bmatrix} x_1 \\ x_2 \\ x_3 \\ x_4 \end{bmatrix}, \quad (18)$$

$$\text{so, } \mathbf{H} = \begin{bmatrix} 1 & 0 & 0 & 0 \\ 0 & 0 & 1 & 0 \end{bmatrix}. \quad (19)$$

Utilizing a sampler period of T_s seconds and considering a zero order holder, the discrete time state space representa-

tion is (Franklin et al., 1998):

$$\delta \mathbf{x}_{k+1} = \Phi \delta \mathbf{x}_k + \Gamma \delta u_k, \quad (20)$$

$$\mathbf{y}_k = \mathbf{H}(\delta \mathbf{x}_k + \mathbf{x}_0). \quad (21)$$

3. STABILIZING CONTROLLERS

In order to control the system with its linearized model, three major systems characteristics must be dealt: adjust to the fact that the system is linearized to an equilibrium point; there must be a reference signal \mathbf{r} ; and there must be an estimate for the current state \mathbf{x}_k called $\hat{\mathbf{x}}_k$, because not all states are available in system's output.

When the system reaches the reference signal, the control signal will not always be zero, so it has a steady state value u_{ss} , where $\mathbf{f}(\mathbf{r}, u_{ss}) = 0$. So:

$$u_{ss} = u_0 + \delta u_{ss}. \quad (22)$$

In other words, the control signal δu_k will also have a non-zero steady state value. Then, the system's control law can be as follows:

$$\delta u_k = -\mathbf{K}(\delta \mathbf{x}_k - \delta \mathbf{x}_r) + \delta u_{ss}, \quad (23)$$

$$u_k = u_0 - \mathbf{K}(\delta \mathbf{x}_k - \delta \mathbf{x}_r) + \delta u_{ss} = u_{ss} - \mathbf{K}(\delta \mathbf{x}_k - \delta \mathbf{x}_r), \quad (24)$$

$$\text{where, } \delta \mathbf{x}_r = \mathbf{r} - \mathbf{x}_0. \quad (25)$$

The *Separation Principle* says that the controller can be designed as all states are available in output. Then it can be added to a system where a estimator is used with no damage to the desired poles location. The matrix \mathbf{K} will be responsible to minimize the cost function in Eq. (26) (Franklin et al., 1998).

$$J' = \lim_{N \rightarrow \infty} \frac{1}{2} \sum_{k=0}^N (\delta \mathbf{x}_k^T \mathbf{Q}_1 \delta \mathbf{x}_k + \delta u_k Q_2 \delta u_k). \quad (26)$$

The coefficients \mathbf{Q}_1 and Q_2 are responsible to weight the importance of respectively $\delta \mathbf{x}$ and δu to the cost function. From Eq. (26) is obtained the *Algebraic Riccati Equation* below, and with its solution can be obtained \mathbf{K} as shown in Eq. (29) (Franklin et al., 1998).

$$\mathbf{S}_\infty = \Phi^T (\mathbf{S}_\infty - \mathbf{S}_\infty \Gamma \mathbf{R}^{-1} \Gamma^T \mathbf{S}_\infty) \Phi + \mathbf{Q}_1, \quad (27)$$

$$\text{where, } \mathbf{R} = Q_2 + \Gamma^T \mathbf{S}_\infty \Gamma, \quad (28)$$

$$\mathbf{K} = \mathbf{R}^{-1} \Gamma^T \mathbf{S}_\infty \Phi. \quad (29)$$

The coefficient Q_2 is a scalar since only one input to the system, while matrix \mathbf{Q}_1 can be determined by Eq. (30).

$$\mathbf{Q}_1 = \rho \mathbf{H}^T \mathbf{H}. \quad (30)$$

In order to obtain the estimate $\hat{\mathbf{x}}_k$, and complete the LQG design, it is used an *Extended Kalman filter* (EKF) applied to the non-linear state space model. The EKF will be responsible for producing a minimum error variance estimate (Welch and Bishop, 2001). Considering \mathbf{w}_k and \mathbf{v}_k process and measurement white noises respectively, and discretizing the system of differential equations in (6) using Euler method, one obtains:

$$\mathbf{x}_k = \mathbf{x}_{k-1} + T_s \mathbf{f}(\mathbf{x}_{k-1}, u_{k-1}) + \mathbf{w}_k, \quad (31)$$

$$= s(\mathbf{x}_{k-1}, u_{k-1}, \mathbf{w}_k), \quad (32)$$

$$\mathbf{y}_k = \mathbf{H} \mathbf{x}_k + \mathbf{v}_k \quad (33)$$

$$= t(\mathbf{x}_{k-1}, u_{k-1}, \mathbf{v}_k). \quad (34)$$

The process and measurement noises' distributions can be represented as Gaussian ones with null expected value and covariance matrices \mathbf{Q} and \mathbf{R} , respectively. The noises can be represented as (Welch and Bishop, 2001):

$$\mathbf{w} \sim N(0, \mathbf{Q}), \quad (35)$$

$$\mathbf{v} \sim N(0, \mathbf{R}). \quad (36)$$

Doing another linearization to Eq. (32) and (34), are obtained the matrices needed to implement the EKF algorithm. The algorithm can be divided in two parts: the *Prediction* one, when a first estimation is made based on the knowledge about the system, and the *Correction* one, responsible to weight the system's innovation ($\mathbf{y}_k - \mathbf{H} \hat{\mathbf{x}}_{k-1}^-$) (Welch and

Bishop, 2001). Figure 4 represents how the algorithm works.

$$\Phi_{k[i,j]} = \frac{\partial s[i]}{\partial x[j]}(\hat{x}_{k-1}, u_{k-1}, 0) = I + T_s \frac{\partial f}{\partial x}(\hat{x}_{k-1}, u_{k-1}), \quad (37)$$

$$W_{k[i,j]} = \frac{\partial s[i]}{\partial w[j]}(\hat{x}_{k-1}, u_{k-1}, 0) = 1, \quad (38)$$

$$H_{k[i,j]} = \frac{\partial t[i]}{\partial x[j]}(\hat{x}_{k-1}, 0) = H, \quad (39)$$

$$V_{k[i,j]} = \frac{\partial t[i]}{\partial v[j]}(\hat{x}_{k-1}, 0) = 1. \quad (40)$$

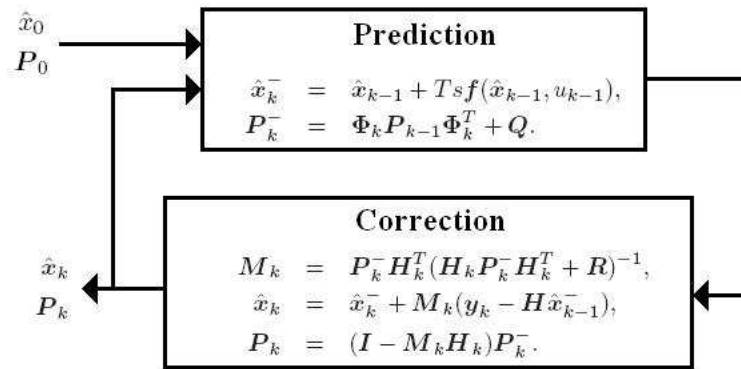


Figure 4. *Extended Kalman filter algorithm.*

4. PHYSICAL SYSTEM PARAMETERS

The construction of a real implementation of a pendubot should consider two system's properties: controllability and observability. Both can be studied with the system's dynamic model, and then, a good set of physical parameters could be found for the real pendulum.

In order to choose in which lengths and material the rotary inverted pendulum's poles are made, there are some facts that should not be ignored: an inverted pendulum with a Link₂ heavier than Link₁ would increase the controllability of the system, although it will imply in a greater control signal; greater lengths would also imply in a greater control signal, but a Link₁ longer than Link₂ would permit the equilibrium to lower values of θ_1 .

The system's control strategy can also be set to help the good behavior of the pendubot. The LQG control uses a local linearized dynamic model to an equilibrium point (x_0, u_0) . It is only accurate when the system's states and input signal do not differ much from the equilibrium values. The use of a very fast controller could take the system out of that region before it gets in steady state, therefore, Q_2 should be greater than ρ (Eq. 30), providing a controlled system that evolves slowly. It happens because the pendubot would have a pole displacement that minimizes the control input u_k .

A good combination of parameters to compose and perform a simulation of a rotary inverted pendulum is shown in Tab. 1. The sampler period T_s is chosen to be 0.001 seconds because it is longer enough to permit the necessary computation time, and permits a good approximation to the real movement that a physical implementation would perform.

Table 1. rotary inverted pendulum parameters used in simulation.

m_1 (kg)	0.3	m_2 (kg)	0.5
l_1 (m)	0.3	l_2 (m)	0.3
d_1 (N.m.s)	0.01	d_2 (N.m.s)	0.01
x_{10} (rad)	$\frac{\pi}{4}$	x_{20} (rad/s)	0
x_{30} (rad)	$\frac{\pi}{2}$	x_{40} (rad/s)	0
$x_{1\ final}$ (rad)	$3\frac{\pi}{4}$	$x_{2\ final}$ (rad/s)	0
$x_{3\ final}$ (rad)	$\frac{\pi}{2}$	$x_{4\ final}$ (rad/s)	0
T_s (rad)	0.001		

As shown in Tab. 1, the controller must bring the rotary inverted pendulum from a state x_0 to x_{final} . To make it possible, several local linearizations to the system are made to get to the desired final state. Consequently, the reference r will evolve to finally be equal to x_{final} . For each linearized model, r will not be more than $\frac{\pi}{36}$ away from the equilibrium point where the linearization was made.

The coefficients Q_1 and Q_2 must be tuned to obtain the control gain K . As mentioned before, a good option would be to set Q_2 greater than ρ . The matrix Q_1 can be obtained from H as follows:

$$Q_1 = \rho H^T H = \rho \begin{bmatrix} 1 & 0 & 0 & 0 \\ 0 & 0 & 0 & 0 \\ 0 & 0 & 1 & 0 \\ 0 & 0 & 0 & 0 \end{bmatrix}. \quad (41)$$

And Q_2 is just a constant:

$$Q_2 = \eta. \quad (42)$$

A good combination for ρ and η used in simulation is $\rho = 1$ and $\eta = 10$.

The adjustment of covariation matrices P_0 and Q is tricky. A good approach would be to minimize the variance of states that cannot be directly measured from the output. Eq. (43) shows the value used for the simulation.

$$P_0 = Q = \begin{bmatrix} 1 & 0 & 0 & 0 \\ 0 & 0.1 & 0 & 0 \\ 0 & 0 & 1 & 0 \\ 0 & 0 & 0 & 0.1 \end{bmatrix}. \quad (43)$$

Considering that both angular sensors used in the real implementation will have a error variance of $\frac{\pi}{1620}$, matrix R equals to:

$$R = \begin{bmatrix} \frac{\pi}{1620} & 0 \\ 0 & \frac{\pi}{1620} \end{bmatrix}. \quad (44)$$

The simulations results are shown in next section.

5. SIMULATION RESULTS

Figures 5(a), 5(b) and 5(c) were obtained from a rotary inverted pendulum simulator programed in MATLAB, and represent the obtained values for θ_1 , θ_2 and u_k respectively. As can be seen, the reference for θ_1 evolves until it reaches the desired value from Tab. 1. Figures 6(a), 6(b) and 6(c) represent the obtained values for θ_1 , θ_2 and u_k respectively but now for a simulation that uses not advised values for poles lengths and weights. As it can be seen, the major value that the control input has achieved is $1.6956 Nm$, that would be the minimum value that a DC motor used in a real experiment could provide. The results show that a rotary inverted pendulum with those characteristics would not be easily controlled and would oscillate when it reaches a value close to the final reference at $\frac{3\pi}{4}$ rad. In fact, a rotary inverted pendulum with $m_2 = 0.1kg$ could not be controlled to follow the references used for both simulations.

Figure (7) shows the simulator interface. With this interface it possible for the user to chose among others control strategies and configurations. For instance, in a given configuration the optimal controller uses the real state vector instead of using the EKF.

6. CONCLUSIONS

In this paper, it has been shown a simulation-based design of a rotary inverted pendulum. Indeed, an optimal regulator has been proposed, but the major result of the analyzed simulation is the control signal maximum value. That clearly is an information that only the simulation could provide in order to aid the choice of physical components of the pendulum. There are many other possibilities for each parameter to the physical implementation, and for each one of them it can be studied how the control setting would perform, whether the physical configuration maximizes or minimizes the controllability, and whether a DC motor with a limited torque could perform the control. One major drawback is the limitation that the linearized model implies for control purpose. A non-linear control could solve this problem, and is one of the ongoing researches topics, such: Markov jump non-linear systems modeling to control the "swing up" mode, and closed-loop identification of the real system.

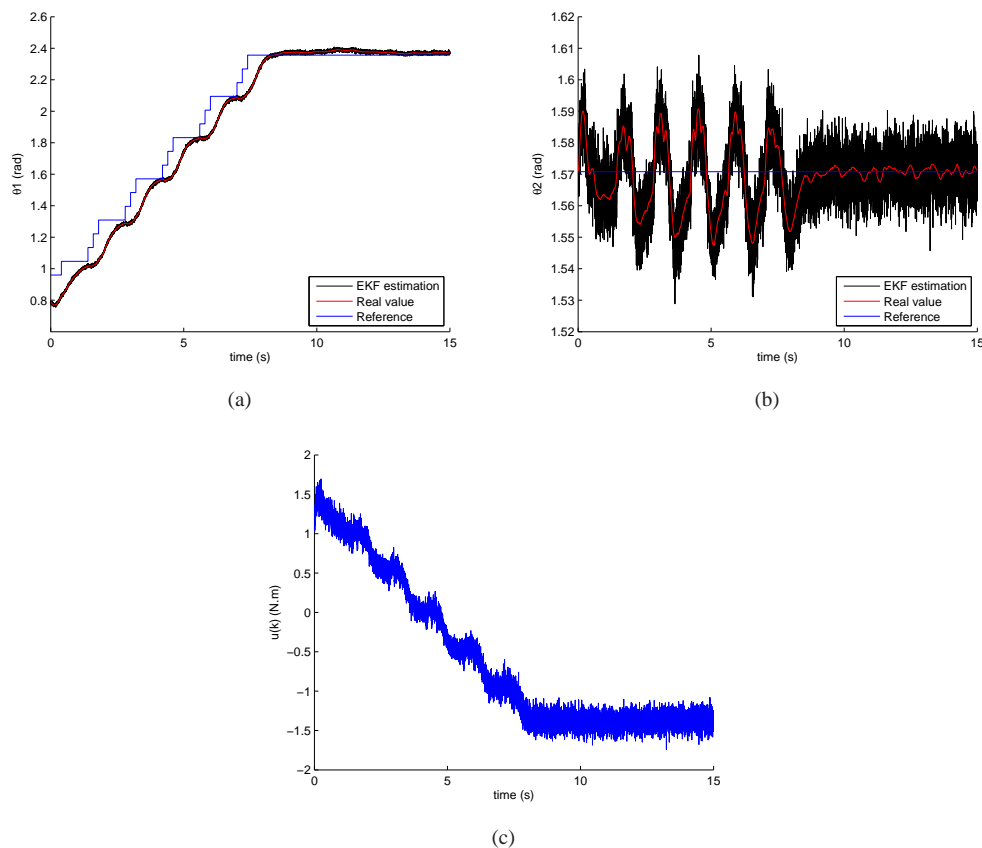


Figure 5. Graphics (a),(b) and (c) are respectively the obtained values for θ_1 , θ_2 and u for a simulation with parameters from Tab. 1, $\rho = 1$ and $\eta = 10$.

7. REFERENCES

References

- Awtar, S., King, N., Allen, T., Bang, I., Hagan, M., Skidmore, D., Craig, K., 2002. Inverted pendulum systems: rotary and arm-driven - a mechatronic system design case study. *Mechatronics* 12, 357–370.
- Franklin, G. F., Powell, J. D., Workman, M., 1998. *Digital Control of Dynamic Systems*. Vol. 3. Addison Wesley Longman, Inc.
- Horáček, P., 2000. Laboratory experiments for control theory courses: A survey. *Annual Reviews in Control* 24, 151–162.
- Merian, L. G., Kraige, L. G., 1999. *Mecânica, Dinâmica*, 4th Edition. LTC.
- Press, W. H., Flannery, B. P., Teukolsky, S. A., Vetterling, W. T., 1992. *Numerical Recipes in C*. Cambridge University Press.
- Spong, M. W., Block, D. J., December 1995. The pendubot: A mechatronic system for control research and education. *IEEE CDC* 34, 555 – 557.
- Stachowiak, T., Okada, T., 2006. A numerical analysis of chaos in the double pendulum. *Chaos, Solutions and Fractals* 29, 417–422.
- Welch, G., Bishop, G., Agosto 2001. An introduction to the kalman filter. *SIGGRAPH* 2001.
- Zhou, Z., Whiteman, C., 1996. Motions of a double pendulum. *Nonlinear Analysis, Theory, Methods & Applications* 26, 1177–1191.

8. Responsibility Notice

The authors are the only responsible for the printed material included in this paper.

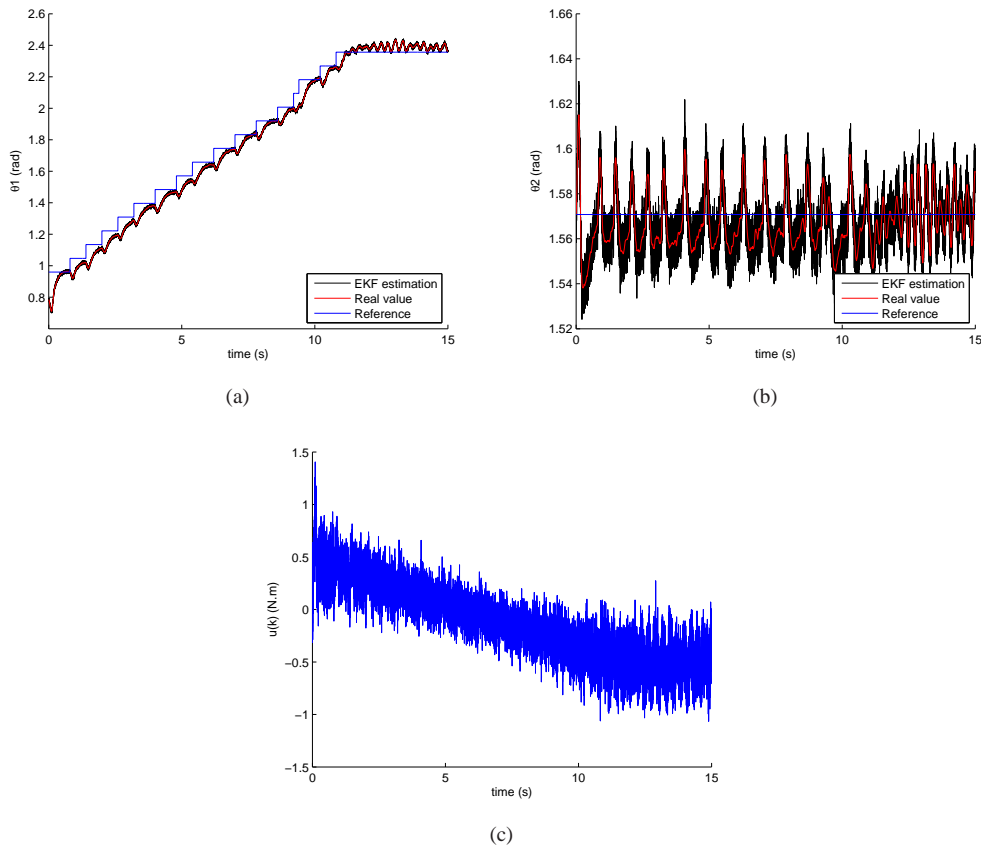


Figure 6. Graphics (a),(b) and (c) are respectively the obtained values for θ_1 , θ_2 and u for a simulation with $l_1 = 0.2m$, $l_2 = 0.3m$, $m_1 = 0.3kg$, $m_2 = 0.2kg$, $\rho = 10$ and $\eta = 1$.

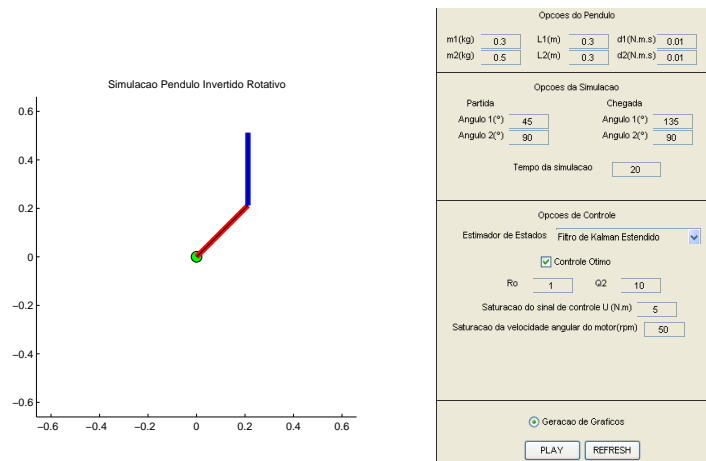


Figure 7. Simulator Interface.